Thermal conductivity of $CeAuAl_3$: Evidence of phonon scattering by Ce magnetic moment fluctuations

Y. Aoki
Laboratorium für Festkörperphysik, Eidgenössische Technische Hochschule-Hönggerberg, 8093 Zürich, Switzerland and Department of Physics, Tokyo Metropolitan University, Hachioji, Tokyo 192-0397, Japan

M. A. Chernikov and H. R. Ott
Laboratorium für Festkörperphysik, Eidgenössische Technische Hochschule-Hönggerberg, 8093 Zürich, Switzerland

H. Sugawara and H. Sato
Department of Physics, Tokyo Metropolitan University, Hachioji, Tokyo 192-0397, Japan
(Received 4 November 1999)

We have measured the thermal conductivity $\lambda(T)$ on tetragonal $CeAuAl_3$ single crystals along both the *a* and *c* axes between 0.4 and 40 K. For comparison, the same measurement has been made on a polycrystalline sample of $LaAuAl_3$. The thermal conductivity of the Ce compound is lower than for the La compound and only weakly anisotropic. No distinct anomalies in $\lambda(T)$ of $CeAuAl_3$ are observed at the antiferromagnetic transition and, far below the Néel temperature, the Wiedemann-Franz law is almost fulfilled. For both compounds a maximum in λ/T, owing to the phonon contribution, has been observed in the vicinity of 10 K. The data are interpreted by considering phonon scattering processes involving the localized $4f$ electron states on the Ce ions.

The magnetic susceptibility and specific heat measured on polycrystalline samples of $CeAuAl_3$ (Ref. 1) have shown that this compound undergoes an antiferromagnetic (AF) transition at $T_N = 1.32$ K. The ordered state involves the following interesting characteristics, which may well be attributed to the presence of strongly correlated electrons in the magnetically ordered state. Well below T_N, the specific heat C_p contains a large linear-in-T term with a coefficient $\gamma = 227\,\mathrm{mJ/(mol\,K^2)}$. The electrical resistivity $\rho(T)$ may be represented by $\rho(T) = \rho_0 + AT^2$, with a large prefactor $A = 5.0\,\mu\Omega\,\mathrm{cm/K^2}$.[1] These facts suggest the presence of moderately mass-enhanced electrons even in the magnetically ordered state. From a ^{27}Al nuclear magnetic resonance (NMR) study,[2] the Ce magnetic moments are estimated to be reduced by ~25% at 50 mK, most likely due to Kondo screening. The magnetic structure of the ordered state is suggested to be of a simple spiral type along the *c* axis with the ordered Ce moments arranged ferromagnetically within the *ab* planes of the tetragonal crystal lattice.[2]

After our success at growing single-crystalline samples, some aspects of the anisotropy in the magnetic and transport properties have been clarified.[3] The electrical resistivity ρ for the current **J** flowing along the *c* axis shows a small increase below T_N while ρ for $\mathbf{J}//a$ axis clearly decreases. This observation indicates the formation of a superzone gap along the *c* axis upon magnetic ordering, which is consistent with the magnetic structure suggested by the NMR data. The magnetic susceptibility shows a clear anisotropy for different orientations of the externally applied magnetic field, i.e., for the $B//a$ and $B//c$ axes. This can be well explained by considering crystalline electric field (CEF) effects. In the derived CEF level scheme, the ground state of the $4f$ magnetic moment is the $J_z = \pm 1/2$ doublet state and the first excited state ($\pm 3/2$ with a small admixture of $\pm 5/2$) is located ~60 K above the ground state.

To gain further insight into the magnetism of the $4f$ electrons involved in this system, we have measured the thermal conductivity using single crystalline samples.

A single-crystal ingot of $CeAuAl_3$ was grown by the Czochralski pulling method with a tetra-arc furnace using high-purity elemental metals (99.99% pure cerium, 99.99% pure gold, and 99.999% pure aluminum). The grown single crystal was subsequently annealed for 2 weeks in vacuum at 700 °C. Two bar-shaped samples were cut from the annealed single crystal using a spark cutter with orientations such that thermal conductivity measurements with the heat flow $\dot{\mathbf{Q}}$ along the *a* and *c* axes, respectively, were possible. The sample dimensions were approximately $1.9\times1.6\times1.4\,\mathrm{mm^3}$ for the $\dot{\mathbf{Q}}//a$ axis and $4.5\times1.0\times0.4\,\mathrm{mm^3}$ for the $\dot{\mathbf{Q}}//c$ axis. Naturally, the heat flow was driven along the longest dimension. The residual electrical resistivities ρ_0 of the samples, as deduced from our low-temperature electrical resistivity $\rho(T)$ data, were 17 and 35 $\mu\Omega$ cm along the *a* and *c* axes, respectively. The slight differences in ρ_0 between the present samples and those in Ref. 3 may be attributed to the uncertainty in the geometrical factors and the difference in the sample quality. In order to examine the quality of the present sample, the specific heat was measured using an adiabatic heat-pulse method by using a dilution refrigerator. As a reference material, polycrystalline $LaAuAl_3$ was synthesized by arc melting and exposed to the same subsequent annealing procedure as the $CeAuAl_3$ single crystal. For $LaAuAl_3$, ρ_0 was 38 $\mu\Omega$ cm.

The thermal conductivity $\lambda(T)$ was measured using a conventional steady-state heat-flow technique between 0.4 and 40 K by using both a ^{3}He and a ^{4}He cryostat. The samples were mounted using silver epoxy between a heater, made of manganin wire wound around a small copper rod,

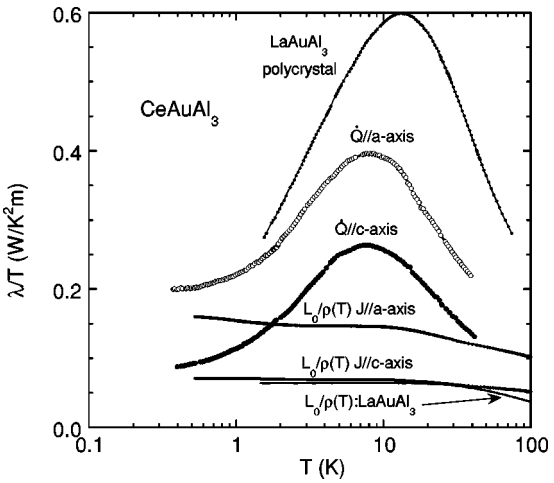

FIG. 1. Temperature dependence of the thermal conductivity of $CeAuAl_3$ (for $\dot{\mathbf{Q}}//a$ axis and $\dot{\mathbf{Q}}//c$ axis) and of $LaAuAl_3$ plotted as λ/T vs T. For comparison, the electrical conductivity of $CeAuAl_3$ (for $\mathbf{J}//a$ axis and $\mathbf{J}//c$ axis) and of $LaAuAl_3$ is also shown as L_0/ρ vs T in the same figure.

and a copper sink, which could be held at constant temperature by a temperature controller. The thermometers used for measuring the established temperature gradients along the samples were Allen-Bradley carbon resistors and Matsushita carbon resistors above and below 2 K, respectively. Flattened gold wires of 0.1 mm diameter were wrapped around the resistors that had been ground to a thickness of approximately 0.2 mm and set in Stycast 2850 epoxy. The extensions of the wires were fixed with silver epoxy at points 0.3 mm from the sample ends. To minimize the heat leak, each thermometer connection was made with long manganin wires of 0.05 mm diameter. Heat leaks by conduction through the heater and the thermometer wires and radiation are estimated to not have exceeded 0.1% of the heat conduction through the sample in the whole temperature range of this experiment. The temperature differences between the two thermometers were kept to about 6% of the mean sample temperature.

The electrical resistivities $\rho(T)$ were measured on the same samples after the thermal conductivity measurements, using the heater and sink as current probes and the gold wires, thermally coupling to the thermometers, as voltage probes. In this way, the geometrical factor is the same for both types of measurements. Therefore, the uncertainty in the geometrical factor ($\sim 5\%$) is not expected to affect the accuracy of the product $\lambda\rho$.

The results of the thermal conductivity (λ) measurements on the $CeAuAl_3$ single crystals and the $LaAuAl_3$ polycrystal are shown in Fig. 1, where λ/T is plotted as a function of $\log(T)$. The most prominent features in Fig. 1 are broad peaks at $T_p = 13\,\mathrm{K}$ for $LaAuAl_3$ and at $T_p = 8\,\mathrm{K}$ for $CeAuAl_3$, respectively. We assume that the experimental values of λ can be described by the sum of two terms

$$\lambda = \lambda_{ph} + \lambda_e, \tag{1}$$

where λ_{ph} and λ_e are contributions to the heat conduction by phonons and electrons, respectively. For a rough estimate of λ_e, we used the Wiedemann-Franz law[4]

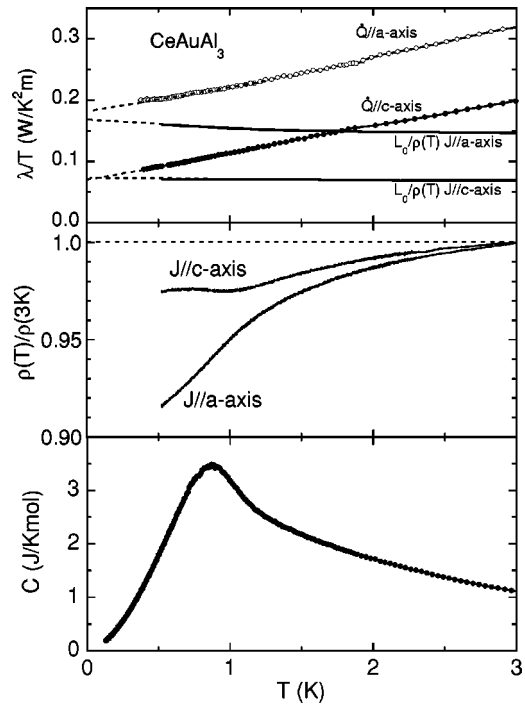

FIG. 2. Temperature dependence of thermal conductivity λ/T, normalized resistivity $\rho(T)/\rho(3\,\mathrm{K})$, and specific heat $C(T)$ of the present sample below 3 K. The dashed lines in λ/T vs T demonstrate linear extrapolations to $T=0$.

$$\lambda_e/T = L_0/\rho, \tag{2}$$

where $L_0 = 2.45\times10^{-8}\,\mathrm{W\Omega\,K^{-2}}$ (the Lorenz number). The temperature variation of L_0/ρ, which is also shown in Fig. 1, is much weaker than that of λ/T. Around T_p, L_0/ρ represents a minor contribution to λ/T; the ratio of L_0/ρ to λ/T at T_p is 0.36, 0.26, and 0.11 for $CeAuAl_3$ ($\dot{\mathbf{Q}}//a$ axis), $CeAuAl_3$ ($\dot{\mathbf{Q}}//c$ axis), and $LaAuAl_3$, respectively. These ratios indicate that the observed peak structure in λ/T is mainly due to phonon heat conduction. The value of T_p is an order of magnitude smaller than the Debye temperature $\Theta_D = 340\,\mathrm{K}$, estimated from the phonon specific heat of $LaAuAl_3$ [$C_{ph} = 0.24\times T^3\,\mathrm{mJ/(K\,mol)}$].[1] In this temperature range ($T/\Theta_D \sim 0.1$), λ_e is expected to fall to some extent below the value implied by the Wiedemann-Franz law because of the inelastic electron scattering by phonons.[5] However, this effect does not seriously affect the above conclusion since the term λ_{ph}/T is obviously dominating.

Figure 2 shows the temperature variations of λ/T, ρ, and the specific heat (C) at low temperatures below 3 K. A clear peak in $C(T)$ evidences the AF phase transition at $T_N = 0.9\,\mathrm{K}$, which is somewhat lower than the value reported for a polycrystalline sample (1.32 K).[1] A similar situation with T_N lower for a single-crystalline sample than for a polycrystalline specimen was also reported for $CeCuAl_3$.[6] The resistivity for $\mathbf{J}//c$ axis first increases with decreasing temperature below 1 K in contrast to the continuous decrease of ρ for $\mathbf{J}//a$ axis. This anisotropy of the electrical resistivity below T_N indicates the opening of a gap on parts of the Fermi surface in the direction along the c axis, caused by the AF phase transition. Around T_N, no distinct anomaly in the form of a cusp structure, theoretically expected in the vicin-

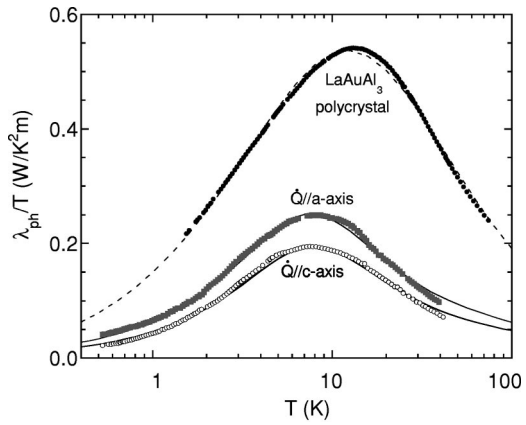

FIG. 3. Estimated phonon thermal conductivity λ_{ph}/T as a function of T. The dashed and solid curves represent the best model fittings (see text).

ity of spin-density-wave transition temperatures,[7] can be seen in λ/T. This is not surprising because the expected anomaly in λ_e/T is only a few percent of the total measured value[7] and cannot be resolved with our experimental resolution. This observation implies that only a small portion of the Fermi surface, which is perpendicular to the c axis, is involved in the superzone gap formation associated with the phase transition. We speculate that the rest of the Fermi surface may contribute to the heavy-electron behavior. At T_N, λ_{ph} accounts for $\sim 25\%$ and $\sim 35\%$ of λ for $\dot{\mathbf{Q}}//a$ axis and $\dot{\mathbf{Q}}//c$ axis, respectively. Any anomaly in λ_{ph} at T_N is also expected to be small, as will be discussed below. Below 3 K λ/T decreases almost linearly down to the lowest reached temperatures; i.e., λ can roughly be described as

$$\lambda \simeq a_1 T + a_2 T^2. \tag{3}$$

As demonstrated in this figure, the λ/T value extrapolated to $T=0$ is almost the same as that for L_0/ρ. Therefore we conclude that, in the limit of $T \to 0$, the first term in Eq. (3) is mainly due to the electronic contribution (λ_e) and the Wiedemann-Franz law is almost fulfilled; i.e., the elastic scattering of electrons must be dominating at very low temperatures.

Figure 3 shows λ_{ph}/T as a function of temperature, calculated using Eqs. (1) and (2). The ratio λ_{ph}/T for $\dot{\mathbf{Q}}//a$ axis, referred to as λ^a_{ph}/T, is larger than λ^c_{ph}/T. In the measured temperature range, both λ^a_{ph}/T and λ^c_{ph}/T are much smaller than λ_{ph}/T for $LaAuAl_3$. The large suppression in λ_{ph}/T for $CeAuAl_3$, much larger than the anisotropy, is most probably due to the scattering of phonons due to $4f$ magnetic-moment fluctuations, as discussed below.

In the case where at low temperatures the phonon scattering is dominated by diffuse scattering at the sample surface, λ_{ph} is estimated to be $\sim C_{ph} v_s l_s/3$, where C_{ph}, v_s, and l_s represent the phonon specific heat, the average sound velocity, and the sample size, respectively.[8] If we use the experimentally established values $C_{ph}=0.24\times10^{-3}T^3$ J/(K mol),[1] $v_s=3\times10^3$ m/s (3.17×10^3 m/s for longitudinal waves along the a axis has been obtained by a sound velocity measurement[9]), and $l_s=1$ mm, we calculate λ_{ph}/T to be about two orders of magnitude larger than the experimental value at 1.5 K. This clearly means that the phonon mean free path is not limited by the sample size.

To analyze the phonon scattering in more detail, we use a Debye-type relaxation-time approximation.[4] The lattice contribution to the thermal conductivity is thus given by

$$\lambda_{ph}(T) = \frac{k_B}{2\pi^2 v_s}\left(\frac{k_B T}{\hbar}\right)^3 \int_0^{\Theta_D/T} \tau(xT)\frac{x^4 e^x}{(e^x-1)^2}dx, \tag{4}$$

where $x=\hbar\omega/k_B T$, Θ_D is Debye temperature, and $\tau(xT=\hbar\omega/k_B)$ is the frequency-dependent relaxation time of phonons. For simplicity, v_s is assumed to be constant. Assuming Matthiessen's rule for phonon scattering rates, τ for $LaAuAl_3$ (τ_0) may be represented by

$$\tau_0^{-1}(\hbar\omega/k_B) = c_0 + c_1(\hbar\omega/k_B) + c_2(\hbar\omega/k_B)^2 + c_4(\hbar\omega/k_B)^4. \tag{5}$$

Here, c_0, c_1, c_2, and c_4 are related to the strengths of phonon scattering by grain boundaries, dislocations, or electron-phonon scattering processes, sheetlike faults, and point defects (ω^4-Rayleigh scattering), or three-phonon scattering processes, respectively.[4] Note that generally an $(\hbar\omega/k_B)^n$ term of τ_0 in Eq. (5) leads to a T^{3-n} dependence of λ_{ph}. By a least-squares fitting with Eqs. (4) and (5), we obtained the energy dependence of τ_0 from the $\lambda_{ph}(T)$ data of $LaAuAl_3$. The result is reliable in a limited energy range corresponding to the limited temperature range of the $\lambda_{ph}(T)$ data. The term $(x^4e^x)/(e^x-1)^2$ in Eq. (4) has a broad peak at $x\simeq3.8$, which means that, at a given T, phonons with an energy of $\hbar\omega\simeq3.8k_BT$ give the largest contribution to λ_{ph}. Therefore, the derived energy dependence of τ_0 is meaningful in the energy range between $\hbar\omega/k_B\sim5$ K and ~300 K, which corresponds to the experimentally covered temperature range from 1.5 K to 80 K. The best fitting ($c_0\simeq0$ s^{-1}, $c_1=6.4\times10^{10}$ K^{-1} s^{-1}, $c_2=3.7\times10^9$ K^{-2} s^{-1}, and $c_4=1.6\times10^6$ K^{-4} s^{-1}) is shown in Fig. 3 and is represented by the dashed curve. The dominant terms in τ_0^{-1} are $(\hbar\omega/k_B)^1$ for $\hbar\omega/k_B<10$ K and $(\hbar\omega/k_B)^4$ for $\hbar\omega/k_B>60$ K. The appearance of the maximum in λ_{ph}/T as a function of temperature corresponds to the crossover between the two energy regions.

Although the overall behavior of λ_{ph}/T of $CeAuAl_3$ looks qualitatively similar to that of $LaAuAl_3$, the Ce compound obviously suffers from enhanced scattering rates, especially in the high-temperature (high-energy) region. The same analysis as made for $LaAuAl_3$ leads to $c_4=1.9\times10^7$ K^{-4} s^{-1} for $\dot{\mathbf{Q}}//a$ axis of $CeAuAl_3$, which is one order of magnitude larger than for $LaAuAl_3$. However, it is unlikely that the single-crystalline $CeAuAl_3$ samples exhibit a higher density of point defects or possess higher phonon-phonon scattering rates than for polycrystalline $LaAuAl_3$. The lower value of the residual resistivity in $CeAuAl_3$ (see L_0/ρ in Fig. 1) supports this assumption. We therefore suggest that the enhanced scattering rate in $CeAuAl_3$ is mainly due to phonon scattering by fluctuating $4f$ magnetic moments.

To analyze the magnetic phonon scattering, we assume that the direct processes of the resonant scattering mechanism proposed by Orbach[10] are dominating. In our model, the magnetic scattering rate (τ_{mag}^{-1}) is described by the sum

of two terms, i.e., the formula derived by McClintock and Rosenberg[11] with an extension to include the contribution from the second-excited CEF doublet, and $c_m(\hbar\omega/k_B)^1$. Noted that the second term, dominating below 10 K, is necessary for reproducing the experimental data, indicating that the electron-phonon scattering rate is enhanced for $CeAuAl_3$ compared to $LaAuAl_3$, probably related to the heavy-fermion state. The existence of this term, leading to a T^2 dependence of λ_{ph} at low temperatures, is consistent with the interpretation that the second term in Eq. (3) is due to the phonon heat conduction. Following Matthiessen's rule, τ^{-1} for $CeAuAl_3$ is then given by $\tau_{mag}^{-1}+\tau_0^{-1}$. The fitting parameters in τ_{mag}^{-1} are c_m, the averaged phenomenological spin-phonon (orbit-lattice) matrix element ($\mathcal{H}_{ol}$), the energy levels of the two CEF excited doublets (D_1 and D_2), and the effective Gaussian width of these levels (Δ).[11] In Fig. 3, the best fits are shown by the solid curves for $CeAuAl_3$, which reproduce the data fairly well. The obtained values are $c_m=1.0\times10^{11}$ (1.7×10^{11}) $K^{-1}\,s^{-1}$, $\mathcal{H}_{ol}=1000$ (1700) K, $D_1=69$ (78) K, $D_2=180$ (210) K, and $\Delta=13$ (16) K for $\dot{\mathbf{Q}}//a$ axis ($\dot{\mathbf{Q}}//c$ axis). The values of D_1 are not far from ~60 K estimated from the magnetic susceptibility data.[1,3] In this model, T_p for $CeAuAl_3$ is sensitive to varying D_1, and the lower T_p for $CeAuAl_3$ compared to that for $LaAuAl_3$ is a consequence of the resonant scattering dominating at higher temperatures. In Fig. 1, $L_0/\rho(T)$ for $CeAuAl_3$ starts to decrease above $\sim T_p$ with increasing temperature. This is most probably caused by conduction-electron scattering due to the excitations in the $4f$ electron system.

Based on the ^{27}Al NMR measurements,[2] the magnetic structure of the ordered state has been suggested to be of a simple spiral type with the ordered Ce moments arranged ferromagnetically within the ab planes of the tetragonal crystal lattice. In this model, the Ce moment direction rotates by 100° from one ab plane to the next along the c axis, i.e., the modulation period being about 20 Å along the c axis. Assuming $v_s=3\times10^3$ m/s,[9] the wavelength of the thermally excited phonons contributing the most to the heat conduction is estimated to be about $\lambda_{th}=200$ Å at $T=T_N$, i.e., much larger than the modulation period even at T_N and increasing further with decreasing temperature. This might be the reason why the magnetic ordering does not affect the phonon heat conduction in any significant way.

In summary, we have measured the thermal conductivity $\lambda(T)$ on $CeAuAl_3$ single crystals between 0.4 and 40 K. Above ~2 K, the phonon contribution (λ_{ph}) is dominating and λ_{ph}/T shows a pronounced broad peak at $T_p\sim10$ K. The lower T_p as well as the overall lower thermal conduction for $CeAuAl_3$, compared to that for $LaAuAl_3$, can be explained by a dominant phonon scattering process by the localized $4f$ electrons, taking into account the CEF level splitting. In the magnetically ordered heavy-fermion state, the electronic contribution (λ_e) is dominating and the Wiedemann-Franz law is almost fulfilled at low temperatures judging from the extrapolation of the temperature variation of λ/T down to $T=0$, indicating that the dominant scattering of the conduction electrons is elastic. In the same regime, the phonon contribution (λ_{ph}) is roughly described by a T^2 dependence. No distinct anomaly in $\lambda(T)$ is seen at the antiferromagnetic transition temperature. In combination with the electrical resistivity data, this implies that only a small portion of the Fermi surface is involved in the superzone gap formation associated with the AF phase transition.

We are grateful to H. Thomas for technical assistance. Y.A. thanks the Swiss National Science Foundation and Japan Society for the Promotion Science for financial support. This work was partly supported by a Grant-in-Aid for Scientific Research from the Ministry of Education, Science and Culture.

[1] S. Paschen, E. Felder, and H.R. Ott, Eur. Phys. J. B **2**, 169 (1998).
[2] P. Vonlanthen, J.L. Gavilano, B. Ambrosini, and H.R. Ott, Eur. Phys. J. B **7**, 9 (1999).
[3] H. Sugawara, S.R. Saha, T.D. Matsuda, Y. Aoki, H. Sato, J.L. Gavilano, and H.R. Ott, Physica B **259-261**, 16 (1999).
[4] R. Berman, *Thermal Conduction in Solids* (Clarendon Press, Oxford, 1976).
[5] I.A. Smirnov and V.S. Oskotski, in *Handbook on the Physics and Chemistry of Rare Earths*, edited by K.A. Gschneidner, Jr. and L. Eyring (Elsevier Science, New York, 1993), Vol. 16, p. 115.
[6] M. Kontani, H. Ido, H. Ando, T. Nishioka, and Y. Yamaguchi, J. Phys. Soc. Jpn. **63**, 1652 (1994).
[7] K. Maki, Phys. Rev. B **46**, 7219 (1992).
[8] H.B.G. Casimir, Physica (Amsterdam) **5**, 495 (1938).
[9] T. Sakashita and M. Yoshizawa (private communication).
[10] R. Orbach, Proc. R. Soc. London, Ser. A **264**, 458 (1961).
[11] P.V.E. McClintock and H.M. Rosenberg, Proc. R. Soc. London, Ser. A **302**, 419 (1968).